ANNALS OF
BOTANY
Founded 1887

Asynchronous leaf and cambial phenology in a tree species of the Congo Basin requires space–time conversion of wood traits

Tom De Mil[1,2,*], Wannes Hubau[2], Bhély Angoboy Ilondea[1,2,3], Mirvia Angela Rocha Vargas[1,4], Pascal Boeckx[4], Kathy Steppe[5], Joris Van Acker[1], Hans Beeckman[2] and Jan Van den Bulcke[1]

[1]UGCT-UGent-Woodlab, Ghent University, Laboratory of Wood Technology, Department of Environment, Coupure Links 653, B-9000 Gent, Belgium, [2]Royal Museum for Central Africa, Wood Biology Service, Leuvensesteenweg 13, B-3080 Tervuren, Belgium, [3]Institut National pour l'Etude et la Recherche Agronomiques, Kinshasa, Democratic Republic of the Congo, [4]Isotope Bioscience Laboratory – ISOFYS, Ghent University, Department of Green Chemistry and Technology, Coupure Links 653, B-9000 Gent, Belgium and [5]Laboratory of Plant Ecology, Department of Plants and Crops, Faculty of Bioscience Engineering, Ghent University, Coupure Links 653, B-9000 Gent, Belgium
*For correspondence Email tom.demil@ugent.be

• **Background and Aims** Wood traits are increasingly being used to document tree performance. In the Congo Basin, however, weaker seasonality causes asynchrony of wood traits between trees. Here, we monitor growth and phenology data to date the formation of traits.
• **Methods** For two seasons, leaf and cambial phenology were monitored on four *Terminalia superba* trees (Mayombe) using cameras, cambial pinning and dendrometers. Subsequently, vessel lumen and parenchyma fractions as well as high-resolution isotopes ($\delta^{13}C/\delta^{18}O$) were quantified on the formed rings. All traits were dated and related to weather data.
• **Key Results** We observed between-tree differences in green-up of 45 d, with trees flushing before and after the rainy season. The lag between green-up and onset of xylem formation was 59 ± 21 d. The xylem growing season lasted 159 ± 17 d with between-tree differences of up to 53 d. Synchronized vessel, parenchyma and $\delta^{13}C$ profiles were related to each other. Only parenchyma fraction and $\delta^{13}C$ were correlated to weather variables, whereas the $\delta^{18}O$ pattern showed no trend.
• **Conclusions** Asynchrony of leaf and cambial phenology complicates correct interpretation of environmental information recorded in wood. An integrated approach including high-resolution measurements of growth, stable isotopes and anatomical features allows exact dating of the formation of traits. This methodology offers a means to explore the asynchrony of growth in a rainforest and contribute to understanding this aspect of forest resilience.

Keywords: Leaf phenology, cambial phenology, parenchyma, vessel lumen, cellulose stable isotopes, Congo Basin, *Terminalia superba*

INTRODUCTION

Future climate change is expected to push tropical ecosystems into novel, unprecedented states (Holm *et al.*, 2017). Therefore, it is vital to understand how this will affect plant growth (Reyer *et al.*, 2013; Cavaleri *et al.*, 2015) in general and forests specifically, given the enormous value of this natural capital. The majority of forest biomass is stored in the wood and bark of trees (Beeckman, 2016) and studying radial growth is therefore imperative (Steppe *et al.*, 2015) given the uncertainties in tropical tree carbon gain and specific vulnerability to drought (Zuidema *et al.*, 2013; Gebrekirstos *et al.*, 2014). Long-term growth, climate response and ecological information can be read from rings in trees.

In tropical trees, the classic matching of ring widths is often not possible due to discontinuous or wedging rings or unclear ring boundaries (Tarelkin *et al.*, 2016), which often result in many uncertainties regarding growth rate and how these trees embed ecological and climate information into their wood

structure. Consequently, there is a clear need for alternative approaches to interpreting and analysing tropical tree rings (Silva *et al.*, 2019). One option is to study wood traits embedded within these rings, to tap into underexplored intra-annual ecological information from the past (Fonti *et al.*, 2010; Battipaglia *et al.*, 2014b; Sass-Klaassen, 2015; Van Camp *et al.*, 2018).

Establishing such high-resolution or intra-annual chronologies (Eckstein, 2004; Rossi and Deslauriers, 2007) of wood traits [which can include elemental (Poussart *et al.*, 2006; Cherubini *et al.*, 2013; Hietz *et al.*, 2015), wood stable isotope (Helle and Schleser, 2004; Verheyden *et al.*, 2004; Poussart *et al.*, 2004; Evans and Schrag, 2004; Fichtler *et al.*, 2010; Managave and Ramesh, 2012) and wood anatomical traits (Fonti *et al.*, 2010; Battipaglia *et al.*, 2010; von Arx *et al.*, 2016)] can reveal climatic control on tree growth and how these traits vary during tree development. Concentrations of cellulose stable isotopes in leaves and wood ($\delta^{13}C$, $\delta^{18}O$) are of particular interest in the tropics, as a proxy for physiological processes such as stomatal

conductance, intrinsic water use efficiency (van der Sleen *et al.*, 2014) and source water use. Especially at the intra-annual level, a clear link with weather conditions such as monsoon rains has been reported (Schollaen *et al.*, 2014).

More and more studies in tropical regions are combining isotope analysis and wood anatomical traits to relate physiological processes to hydraulic properties (Li *et al.*, 2011; Battipaglia *et al.*, 2014*a*). However, weak seasonality causes these traits to be difficult to date. A sound interpretation of growth patterns of tropical trees depends on understanding phenological rhythms (Enquist and Leffler, 2001) at the primary meristem level (leaf phenology) and at the secondary meristem level (cambial phenology). It is therefore essential to study both simultaneously.

Landscape leaf phenology can be studied from satellite images (Ryan *et al.*, 2017) but individual phenology variations are studied using detailed *in situ* field observations (Borchert *et al.*, 2005; Fu *et al.*, 2015) or digital repeat photography (Sonnentag *et al.*, 2012). Cambial phenology, although more difficult to measure, is archived in the secondary xylem (Beeckman, 2016) via radial growth. Monitoring radial growth at high precision in the tropics (Krepkowski *et al.*, 2010; Trouet *et al.*, 2012; Mendivelso *et al.*, 2016; Spannl *et al.*, 2016; Butz *et al.*, 2017; Raffelsbauer *et al.*, 2019) provides a mechanistic understanding of seasonal wood formation as a function of weather variables.

Phenology varies due to climate (Borchert, 1999; Borchert *et al.*, 2005; Lisi *et al.*, 2008; Yáñez-Espinosa *et al.*, 2010; Fauset *et al.*, 2012) and growth strategies (Couralet *et al.*, 2013; Wolfe and Kursar, 2015) at the species and even individual plant levels (Heinrich and Banks, 2006; Forrest and Miller-Rushing, 2010; Visser *et al.*, 2010). Closely linked to leaf phenology variability, the exact period of tree ring formation within one growing season varies with age, site (Philipson *et al.*, 1971; Rossi *et al.*, 2008), species and between trees.

Fixing intra-annual wood traits on a seasonal time axis is essential to link the physiological mechanisms (Bouriaud *et al.*, 2005; Steppe *et al.*, 2015; Van Camp *et al.*, 2018) to environmental conditions. The intra-annual curve can be used to convert wood traits to the time domain for some tree species in temperate regions (e.g. Wimmer *et al.*, 2002; Bouriaud *et al.*, 2005; Skomarkova *et al.*, 2006; Stangler *et al.*, 2016) but this combinatory approach is missing for species in the Congo Basin.

Given the challenging task of measuring tree performance in the past, there is a clear need to improve knowledge of xylem responses to climate variability in tropical trees. Intra-annual wood traits should be coupled to the growth rhythms which are determined based on leaf and cambial phenology.

This study reports on *Terminalia superba*, a deciduous tree (Couralet *et al.*, 2013) with good potential for tree-ring analysis

and considerable inter- and intra-annual anatomical variation (De Ridder *et al.*, 2013; De Mil *et al.*, 2016), but for which knowledge on the timing of the latter remains elusive.

Here, we hypothesize that the timing of leaf and cambial phenology are related and determine the synchrony of wood cellulose stable isotope $\delta^{13}C$ and $\delta^{18}O$ and wood anatomical traits. Hence, when these traits are synchronized accordingly by fixing on a time axis through the seasonal growth curve, their common signal could be increased, rather than assessing them in the spatial domain by simple averaging.

MATERIAL AND METHODS

Study site and species

The Luki reserve (5°37.31′S, 13°5.90′E) lies at the southern edge of the Mayombe, which is an Atlantic Coastal forest ranging from Gabon to western DR Congo (Supplementary Data Fig. S1a). The rainy season (average 1188 ± 245 mm) lasts from October to May, yet the dry season is less pronounced due to thick cloud cover and high relative humidity (Lubini, 1997).

Terminalia superba is a widespread pioneer in the Mayombe forest. Its distribution area ranges from Sierra Leone, along the West African coastline, and up to the northern boundary of Angola. The Luki reserve is at the edge of its distribution area. Four trees were selected on different locations around the Nkulapark in the Luki Reserve close to the research station, and monitored from August 2013 to December 2015, covering three season onsets and two full growing seasons. Height (*H*) and diameter (*D*) of the study trees and neighbouring trees were measured and crown area was calculated as well. Subsequently, the crowding index was calculated, as a measure of the influence of neighbouring trees (Michelot *et al.*, 2011) (Table 1; Supplementary Data Fig. S2).

Three-point dendrometers (EcoMatik) were installed on each of the four trees to account for circumferential variation (Supplementary Data Fig. S2d). The dendrometers were installed at 4–5 m height, to reduce the influence of large buttresses. Stem diameter variations (SDVs) were logged every 30 min using ONSETComp HOBOloggers (Onset). Four time-lapse cameras (Wingscapes) (Sonnentag *et al.*, 2012) were installed at 10–20 m height on adjacent trees and directed towards the studied trees for leaf phenology monitoring: two or three pictures per day were taken for two consecutive growing seasons. Time-lapse images were visually analysed and leaf events were classified into defined phenology phases (adapted from Derory *et al.*, 2006). Daily precipitation (*p*, mm) was measured by the local weather station of Luki, and air temperature (*T*, °C), relative humidity (RH, %) and solar radiation (*R*, W m⁻²) were

TABLE 1. *General characteristics of the sampled trees,with label (T), Tervuren Wood identification number at the xylarium (Tw), height (*H*), diameter (*D*), estimated tree age, projected crown area, crowding index (CI) as calculated by* Michelot et al. (2011), *and location and coordinates*

Tree	Tw	*H* (m)	*D* (cm)	Age (years)*	Crown area (m²)	CI (–)	Location	Coordinates
T1	Tw68886	35	47	35	142.5	2.23	Young secondary forest	13.108E, −5.620S
T2	Tw68884	45	69	70	223.2	1.70	Old secondary forest	13.099E, −5.612S
T3	Tw68885	39	65	85	213.6	2.10	Old secondary forest	13.099E, −5.612S
T4	Tw68883	31	83	47	530.0	1.36	Free standing tree, ridge	13.100E, −5.624S

measured and logged with ONSETComp HOBOloggers (U23 and S-LIB-M003 respectively; Onset) near the station with a sampling interval of 30 min. Vapour pressure deficit (VPD) was calculated based on measured *T* and RH in the plant modelling software PhytoSim (Phyto-IT BVBA).

Cambial pinning

Cambial pinning was performed monthly by inserting a needle that wounds the cambium locally. Sampling was done at 0.4–1 m below the point dendrometers in a staggered pattern around the circumference of the tree (Supplementary Data Fig. S1c). Trees were felled and stem discs were harvested in December 2015. Samples of $5 \times 5 \times 5$ cm^3 containing the pinnings were extracted from the discs. All stem discs were given a Tervuren wood (Tw) number for storage in the xylarium. Growth between the previous ring boundary and the cambial wound was measured on fresh samples using a stereo microscope and a Lintab measuring stage in combination with TsapWin software (Rinntech; precision 1: 1000 mm). Relative growth (RG) was then calculated as the distance between the cambial pinning and the previous ring boundary, divided by ring width to cope with the high variability in absolute growth along the circumference (Seo *et al.*, 2007; De Mil *et al.*, 2017).

Vessel lumen fraction, parenchyma fraction and high-resolution isotopes

At the exact position of the point dendrometers, tree rings of the two monitored growing seasons were cut from the stem discs (15 mm × 20 mm), carefully sectioned (Microm HM 440E, thickness 15–25 μm), and cross-sections were stained with safranin and alcian blue to enhance the contrast between the different anatomical components (Jansen *et al.*, 1998).

The cross-sections were imaged on a scanning stage (SCAN 100 × 100, Märzhäuser) with a camera (UC30, Olympus) mounted on a microscope (BX60, Olympus, magnification 5×) and stitched to full images (StreamMotion software, Olympus). Vessel lumina were delineated in ImageJ (Schneider *et al.*, 2012) via manual selection with the magic wand tool, whereas parenchyma was manually indicated using the polygon tool. The vessel lumen fraction and parenchyma area were calculated as a fraction of the total wood cross-sectional area (Supplementary Data Fig. S1e). A pixel-by-pixel radial summation of vessel lumen and parenchyma area was made by dividing by the total width of the section, to obtain fractions. Hence, comparisons with the dendrometer series were made at high spatial resolution.

Intra-annual isotope samples (δ^{13}C and δ^{18}O) were taken adjacent to the point dendrometer positions. A Lintab measuring stage (Rinntech) with a stereomicroscope (SZX 12, Olympus) and a scalpel was used to cut the blocks (15 mm × width of the tree rings) into equal radial slices with an approximate thickness of 0.3 mm to comply with the minimum sample size required for isotope analysis. Cellulose extraction of the radial slices was performed at the ISOFYS Lab, according to a protocol adapted from Wieloch *et al.* (2011). δ^{13}C was measured using

an automated nitrogen carbon analyser – solid and liquids (ANCA-SL, SerCon) interfaced with an isotope ratio mass spectrometer (IRMS) (20-20, SerCon), whereas the same slices were used for δ^{18}O determination using a thermal conversion elemental analyser (Sercon) interfaced with an IRMS (20-20, SerCon). The δ^{13}C and δ^{18}O isotope values are expressed against the international standard Vienna Pee Dee Belemnite and Vienna Standard Mean Ocean Water, respectively. Isotope measurements were not able to be processed from tree T1 over the 2014–2015 growing season.

Isotope and wood anatomical traits were further processed in Matlab r2016b for space–time conversion and statistical analysis. Data are available in Supplementary Data Information S1.

Space/time conversion

Xylem growth onset and cessation were derived from cambial pinning at a monthly resolution. Both onset and cessation were further resolved to a daily time step based on breakpoint correlation analyses (segmented regression) of the SDV series (Supplementary Data Figs S3 and S4).

On some radii of all trees, xylem growth exceeded the measurement range of the dendrometers. Therefore, saturated data were removed and gap-filled using Savitsky-Golay interpolation based on (1) the total tree ring width and (2) cessation dates from the other radii of the same tree which did not show saturation. A smoothed (Savitsky-Golay) curve, eliminating diel variations, was then fitted to the SDV and used to position wood traits on a time axis. All wood trait data were averaged within trees, and synchronized with weather data, followed by resampling to weekly resolution. Pearson correlation analyses were performed between the weekly averaged trait profiles and weather variables.

RESULTS

Leaf phenology

Green-up data are presented in Fig. 1A. Figure 1B includes rainfall data for the end of the dry season and the onset of the following rainy season. Trees show considerable variation in leafing timing up to 45 d (Fig. 1A, Table 2). For all three monitored onsets, flushing occurs either before (T1, T4) or after (T2, T3) the first major rains, except for rain onset in 2015, when all trees flushed before the late onset of rain (Fig. 1B). Unlike leaf flushing, leaf senescence and abscission are not sharply defined in *T. superba* (Supplementary Data Fig. S5). The full deciduous (i.e. leafless) period is short for all trees, ranging from 5 to 25 d. VPD is lowest in the dry season and peaks during the rainy season (Fig. 1C), when radial growth occurs.

Cambial phenology

Wood growth is shown in Fig. 1A for all radii of the four trees during two growing seasons. The original RG series are presented in Supplementary Data Fig. S6.
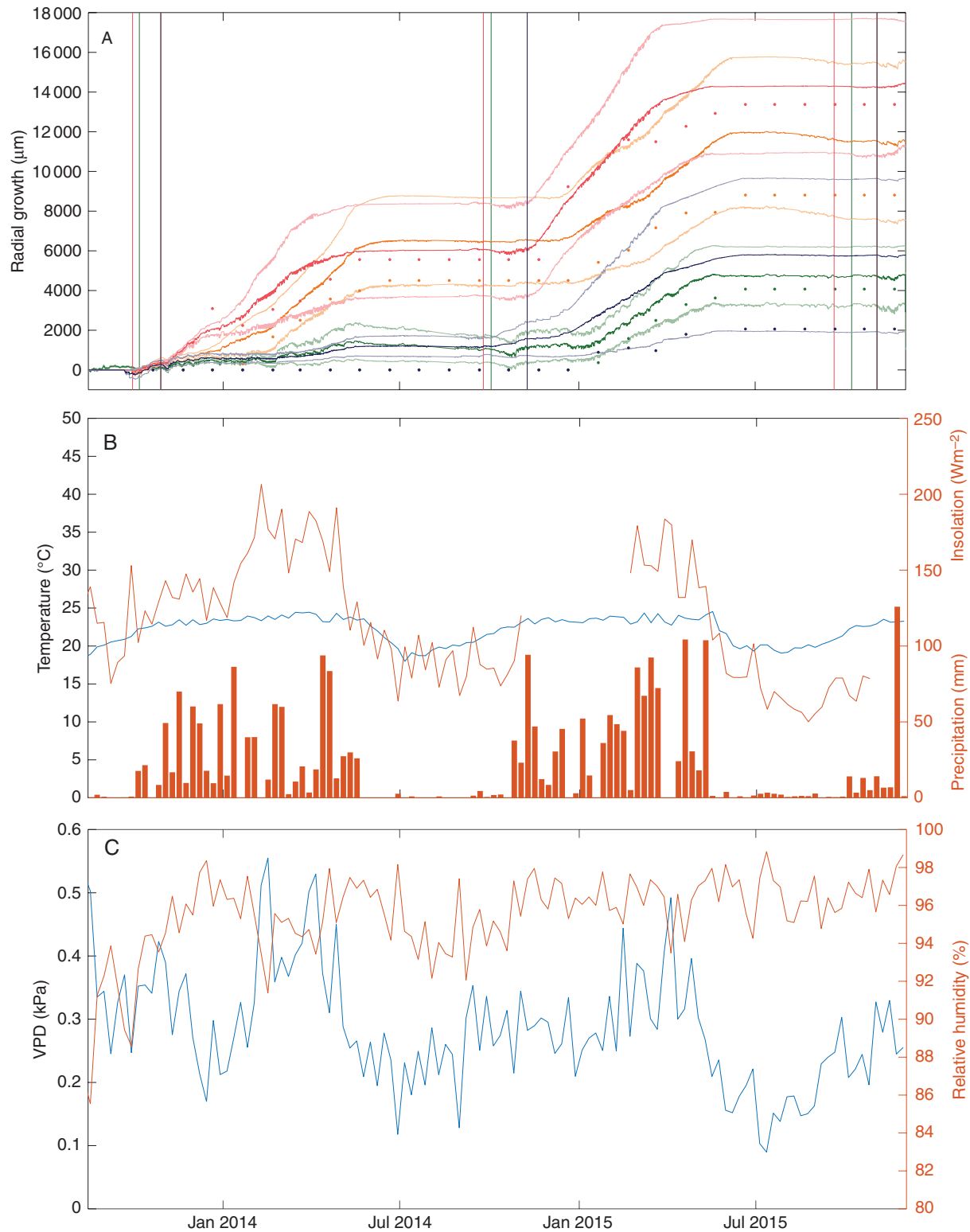
FIG. 1. Comparison of (A) radial growth, cambial pinning data and leaf onset during two seasons of four mature *Terminalia superba* trees in the Mayombe region of the Congo Basin, Central Africa (DR Congo) with (B) mean daily temperature, insolation as well as weekly precipitation for the measured period and (C) vapour pressure deficit (VPD) and relative humidity (RH). Gaps are missing data. In A, full lines are raw radius dendrometer data (three per tree), and each colour represents a tree (T1 green, T2 orange, T3 blue and T4 red). Circles at a given month are growth data derived from cambial pinnings. Vertical lines in A represent bud burst dates from the studied trees.

TABLE 2. *Overview of leaf (Bud burst ± 2 d) and cambial phenology (Onset Xy, ± 5 d) timing (day of the year), the lag between both events and length of the xylem growing season*

Sample	2013–2014					2014–2015					2015–2016		
	Bud burst	Onset Xy	Lag (d)	End Xy	Xy season (d)	Bud burst	Onset Xy	Lag (d)	End Xy	Xy season (d)	Bud burst	Onset Xy	Lag (d)
T1	280	–	–	–	–	276	11	100	138.0	127	280	–	–
T2	302	361	59	154	158	313	359	46	156.0	162	307	–	–
T3	302	–	–	–	–	313	361	48	157.0	161	307	–	–
T4	273	308	35	120	177	268	325	57	130.0	170	263	330	67

Two trees formed no xylem during the 2013–2014 season (indicated by –) and at the time of felling (December 2015) three out of four trees had not yet formed new xylem (see also Supporting Data Fig. S7).

Wood growth starts between November and January for all trees, ranging from 35 to 100 d after bud burst (Table 2). The trees thus start xylem formation well into the wet season. When trees start growing earlier, growth cessation starts earlier in all monitored trees and throughout the monitored seasons. On wet sections taken just after tree felling in December 2015, (non-lignified) wood formation could be observed for the early-onset T4 tree, whereas all the other trees did not yet show cambial activity, which confirms the observed differences (Supplementary Data Fig. S7). The onset is identical for the different radii of a tree (Fig. 1A).

Total xylem growing season length is about 159 ± 17 d and is quite constant except for tree T1 with a shorter season of 127 d.

For trees T1 and T3, a missing ring occurred in the 2013–2014 growing season (Fig. 1A, blue and green triangles). The small net growth observed for some radii of these trees in the SDV series is merely due to water status (Fig. 1A), as well as a small amount of wound-induced xylem formation caused by the dendrometer support, which was confirmed visually on the stem discs (Supplementary Data Fig. S8). In the following growing season, these trees formed a ring on all radii.

Wood trait profiles

The $\delta^{13}C$ and $\delta^{18}O$, vessel lumen and parenchyma profiles (Fig. 2) were positioned on a time axis. The lags in trait values can be seen as xylem onsets and cessations are different.

In general, $\delta^{13}C$ increases at the beginning of the growing season, culminates and begins to decrease around February–March (Fig. 2A) with a minimum in June followed by growth cessation. $\delta^{13}C$ values range between −27.11 and −23.28 ‰ and the maximum and minimum intra-annual range within one ring is 3.42 ‰ and 1.76 ‰, respectively. The averaged $\delta^{13}C$ profile is strongly positively correlated with solar radiation, temperature and VPD, and negatively correlated with relative humidity (Table 3). The $\delta^{18}O$ profiles do not show a clear trend for either year in all trees (Fig. 2B), and the values range between 22.59 ‰ and 35.30 ‰ and the maximum and minimum intra-annual range within one ring is 9.24 ‰ and 6.35 ‰, respectively. Parenchyma fractions can locally add up to 45 % of the wood surface, and vessel lumen fractions reach up to 20 %. Due to shifts in the timing of growth, vessels in one tree appear to form 42 d earlier than the other tree and a similar pattern occurs for parenchyma (Fig. 2C, D). Both parenchyma and vessel lumen fractions gradually increase at the beginning of the season, culminate around February, then decrease towards the end of the season. Vessel lumen fractions and parenchyma fractions are positively related to each other as well as to the $\delta^{13}C$ profile (Table 3). None of the traits is significantly correlated with precipitation.

DISCUSSION

Leaf phenology and cambial phenology

Generally, asynchronous leaf and cambial phenology is observed. Pre-rain green-up in southern African systems (Ryan *et al.*, 2017) is shown here for *T. superba*, where leaf flushing occurs before the onset of rain in some trees (Fig. 1A, B). While there are small differences in leaf flushing between seasons, large differences occur between individuals. Leaf onsets per tree for 2013, 2014 and 2015 are similar (Table 2), but considerable differences in rain onset (Fig. 1B) exist. Other drivers such as insolation or photoperiod might thus influence the timing of flushing as well (Borchert *et al.*, 2015), yet do not explain the individual differences. Variations in leaf onset in *T. superba* (Fig. 1) have also been reported (Mariaux, 1969; Couralet *et al.*, 2013).

Intrinsic factors in this study could thus overrule the effect of precipitation: leaf flushing could merely be a consequence of leaf shedding and resulting changes in tree water status (Borchert, 1999). *Terminalia superba* can thus be considered a brevi-deciduous tree, with a short leafless period and flushing following leaf shedding, and stored stem water could cause some trees to flush before the onset of the rainy season (Borchert, 1994) (Supplementary Data Fig. S5a,b). Additionally, an increase in temperature, from July to September (Fig. 1B), could also be of influence. In the specific case of the Mayombe, water loss during the dry season is probably limited due to reduced VPD (Fig. 1C), as well as occult precipitation (Lubini, 1997) (i.e. condensation drops on leaves from fog that cannot be measured with rain gauges), which could also explain the variability in leaf onset due to lower environmental forcing.

The delay between the onset of leaf and onset of cambial phenology (Table 2) can be explained by tree height. At up to 45 m (Table 1), *T. superba* is one of the largest trees in the Mayombe, and cambial triggering hormones need to migrate from crown to stem base. This hypothesis is also proposed for temperate regions (Schmitt *et al.*, 2000). Differences in xylem formation onset between *T. superba* trees were observed by Mariaux (1969) and are presented in Fig. 1A. In
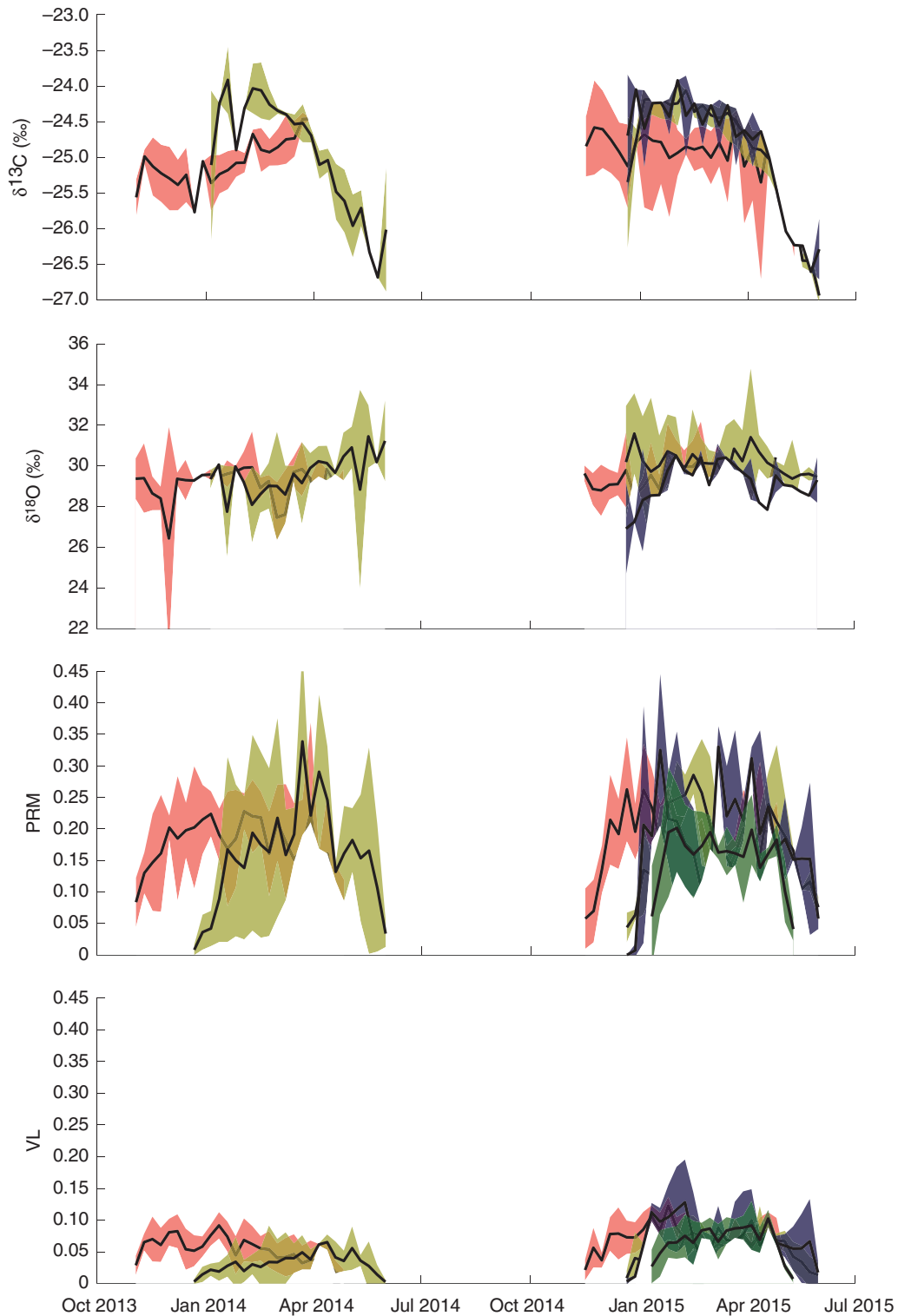
FIG. 2. Synchronized and averaged trait profiles of four *Terminalia superba* trees from Central Africa for (A) cellulose stable δ13C pattern, (B) δ18O pattern, (C) parenchyma fraction (PRM) and (D) vessel lumen fraction (VL). Both fractions are unitless. Each colour represents a tree (T1 green, T2 orange, T3 blue and T4 red) and surface plot shows 1 s.e. Gaps represent the dry seasons. T4 starts developing traits first, while T2 and T3 develop traits further towards the end of the season.

this study, observed differences of up to 50 d are higher than those reported in temperate regions (e.g. Bouriaud *et al.*, 2005; Rossi *et al.*, 2008; Hetzer *et al.*, 2014). Here, we also

report 'live' observation of missing rings in two trees in 2013–2014 (Fig. 2), monitored via SDV and confirmed with cambial pinnings. Based on cambial pinnings, missing rings

TABLE 3. *Pearson correlation matrix of the measured wood traits, and simultaneously measured and calculated environmental variables at a weekly scale*

Variables	$\delta^{13}C$	$\delta^{18}O$	VL	PRM	p	R	RH	T	VPD
$\delta^{13}C$		–0.26	**0.46**	**0.60**	0.23	**0.72**	**–0.55**	**0.59**	**0.56**
$\delta^{18}O$			–0.24	–0.20	–0.08	–0.06	0.15	–0.04	–0.07
VL				**0.60**	0.23	0.27	–0.11	0.15	0.18
PRM					0.05	**0.55**	**–0.41**	**0.49**	**0.44**
p						0.08	0.15	0.10	–0.06
R							**–0.79**	**0.72**	**0.88**
RH								**–0.65**	**–0.90**
T									**0.68**

$\delta^{13}C$ and $\delta^{18}O$, high-resolution isotopes from wood cellulose (‰); VL, vessel lumen fraction (–); PRM, parenchyma fraction (–); p, precipitation (mm); R, solar radiation (W m^{-2}); RH, relative humidity (%); T, temperature (°C); VPD, vapour pressure deficit (kPa). Bold type indicates significant correlations ($P < 0.01$).

were also found in understorey trees of the same study area (De Mil *et al.*, 2017).

Wood traits on a time axis

Intra-annual sampling of individual rings does represent growth increments, but not necessarily equivalent time increments (Poussart *et al.*, 2004), which is confirmed by shifts in time between individual trait profiles (Fig. 2). In order to date $\delta^{13}C$ (Soudant *et al.*, 2016), $\delta^{18}O$ and wood anatomical variables accurately within a tree ring, the space–time conversion approach is used to fix traits of *T. superba* rings on a time axis, and shows that between-tree cambial phenology differences requires shifting of traits to their proper time of formation. Using just spatial averaging per intra-annual position would result in incorrect interpretation of the data.

Large variability in the shape of the $\delta^{13}C$ profiles between trees is also observed for temperate species (Skomarkova *et al.*, 2006; Vaganov *et al.*, 2009; Michelot *et al.*, 2011). Variation between radii (Fig. 2A) of the trees in this study remains largely within general limits of 0.5–1 ‰ (Leavitt, 2010) for $\delta^{13}C$.

The general trend of the intra-annual $\delta^{13}C$ profile for all trees combined (Fig. 2A) is similar for profiles observed in other tropical trees (Verheyden *et al.*, 2004; Poussart *et al.*, 2004; Fichtler *et al.*, 2010). The increase in $\delta^{13}C$ at the onset of the xylem-growing season is due to the use of starch reserves of the previous growing season, which is typically enriched in ^{13}C (Michelot *et al.*, 2011). The decrease towards the end of the growing season is due to the use of current year carbon assimilates to synthesize cellulose (Helle and Schleser, 2004). However, many of these studies assess the isotope pattern as a function of ring position, which makes it difficult to link the isotopic response to specific weather events for interpretation, thus missing the more complete environmental effect that can be seen in the $\delta^{13}C$ profile (Soudant *et al.*, 2016). By synchronizing and linking to weather variables, we obtain a positive relationship between $\delta^{13}C$ and solar radiation and VPD, and a negative relationship with relative humidity (Table 3), which are common environmental factors affecting $\delta^{13}C$ (Managave and Ramesh, 2012).

High-frequency variations are observed in the $\delta^{18}O$ profile (Fig. 2B), without a clear trend. Variation between radii is higher than the general interval 0.5–2 ‰ (Leavitt, 2010). Mixing of water sources (Gessler *et al.*, 2014), a constant high relative humidity (Roden and Siegwolf, 2012), the proximity of the Atlantic Ocean and occult precipitation during the dry season in the Mayombe might cause this variation.

Despite the space–time conversion of the $\delta^{13}C$ and $\delta^{18}O$ and link with weather variables, it is not evident to separate the signal from current-year photosynthesis and remobilization of previous-year storage components (Schleser *et al.*, 1999).

Parenchyma and vessel lumen fractions (Fig. 2C, D) are rarely assessed at an intra-annual scale in trees of the Congo Basin. Vessel lumen fraction is related to $\delta^{13}C$ and parenchyma fraction but has no direct link with weather parameters in this study (Table 3). Vessel lumen area is shown to be positively linked with $\delta^{13}C$ in seasonally dry forests as well (Ohashi *et al.*, 2009).

Parenchyma area (Fig. 2C) is related to vessel area because the axial parenchyma is centred around the vessels (i.e. aliform parenchyma). The main function of parenchyma is storage (Beeckman, 2016; Morris *et al.*, 2016), and while parenchyma is being explored as a climate-sensitive trait (Olano *et al.*, 2013), a mechanistic understanding of its use as a proxy is lacking, especially for axial parenchyma in angiosperms (Eckstein, 2013). A positive correlation between parenchyma and radiation, temperature and VPD, and a negative correlation with relative humidity is observed in this study (Table 3).

To correctly assess the resilience of tropical trees, asynchrony between trees should be further investigated, where more advanced pattern matching of wood traits could offer further prospects (Mann *et al.*, 2018). Given the greater occurrence of extreme climatic events and the potential effect on leaf phenology, variation in tree-specific phenology presented here, as opposed to general phenology trends (Ryan *et al.*, 2017), will impact the interpretation of wood traits considerably, and should be given more emphasis in ecological and biomass (Cuny *et al.*, 2015) modelling of tropical forests.

SUPPLEMENTARY DATA

Supplementary data are available online at https://academic.oup.com/aob and consist of the following. Fig. S1: Study site and illustration of the cambial pinnings, cameras, dendrometers and wood anatomical measurements. Fig. S2: Information on the size and site characteristics of the studied trees. Fig. S3: Scheme of the space–time conversion and breakpoint analysis. Fig. S4: Results of breakpoint analysis for further fine-tuning the date of onset and cessation of xylem formation based on pinning and dendrometer data. Fig. S5: Leaf flushing and leaf shedding events, plotted together with stem diameter variations, at the end of the dry season and the end of the wet season, respectively. Fig. S6: Xylem growth season length of all trees. Fig. S7: Microsections at the beginning of the 2015–2016 season, with cambial stadia visible. Fig. S8: Observation of a missing ring on the stem disc, at the dendrometer position. Information S1: Data link to anatomical sections and data analysis.

LITERATURE CITED

von Arx G, Crivellaro A, Prendin AL, Čufar K, Carrer M. 2016. Quantitative wood anatomy—practical guidelines. *Frontiers in Plant Science* **7**: 781.

Battipaglia G, De Micco V, Brand WA, et al. 2010. Variations of vessel diameter and δ^{13}C in false rings of *Arbutus unedo* L. reflect different environmental conditions. *New Phytologist* **188**: 1099–1112.

Battipaglia G, De Micco V, Brand WA, et al. 2014a. Drought impact on water use efficiency and intra-annual density fluctuations in *Erica arborea* on Elba (Italy). *Plant, Cell & Environment* **37**: 382–391.

Battipaglia G, De Micco V, Sass-Klaassen U, Tognetti R, Mäkelä A. 2014b. Special issue: WSE symposium: Wood growth under environmental changes: the need for a multidisciplinary approach. *Tree Physiology* **34**: 787–791.

Beeckman H. 2016. Wood anatomy and trait-based ecology. *IAWA Journal* **37**: 127–151.

Borchert R. 1994. Soil and stem water storage determine phenology and ditribution of tropical dry forest trees. *Ecology* **75**: 1437–1449.

Borchert R. 1999. Climatic periodicity, phenology, and cambium activity in a tropical dry forest trees. *IAWA Journal* **20**: 239–247.

Borchert R, Renner SS, Calle Z, et al. 2005. Photoperiodic induction of synchronous flowering near the Equator. *Nature* **433**: 627–629.

Borchert R, Calle Z, Strahler AH, et al. 2015. Insolation and photoperiodic control of tree development near the equator. *New Phytologist* **205**: 7–13.

Bouriaud O, Leban J-M, Bert D, Deleuze C. 2005. Intra-annual variations in climate influence growth and wood density of Norway spruce. *Tree Physiology* **25**: 651–660.

Butz P, Raffelsbauer V, Graefe S, et al. 2017. Tree responses to moisture fluctuations in a neotropical dry forest as potential climate change indicators. *Ecological Indicators* **83**: 559–571.

Cavaleri MA, Reed SC, Smith WK, Wood TE. 2015. Urgent need for warming experiments in tropical forests. *Global Change Biology* **21**: 2111–2121.

Cherubini P, Humbel T, Beeckman H, et al. 2013. Olive tree-ring problematic dating: a comparative analysis on Santorini (Greece). *PLoS ONE* **8**: 1–5.

Couralet C, Van Den Bulcke J, Ngoma LM, Van Acker J, Beeckman H. 2013. Phenology in functional groups of central african rainforest trees. *Journal of Tropical Forest Science* **25**: 361–374.

Cuny HE, Rathgeber CBK, Frank D, et al. 2015. Woody biomass production lags stem-girth increase by over one month in coniferous forests. *Nature Plants* **1**: 15160.

De Mil T, Vannoppen A, Beeckman H, Van Acker J, Van den Bulcke J. 2016. A field-to-desktop toolchain for X-ray CT densitometry enables tree ring analysis. *Annals of Botany* **117**: 1187–1196.

De Mil T, Angoboy Ilondea B, Maginet S, et al. 2017. Cambial activity in the understory of the Mayombe forest, DR Congo. *Trees - Structure and Function* **31**: 49–61.

De Ridder M, Trouet V, Van den Bulcke J, Hubau W, Van Acker J, Beeckman H. 2013. A tree-ring based comparison of *Terminalia superba* climate-growth relationships in West and Central Africa. *Trees - Structure and Function* **27**: 1225–1238.

Derory J, Léger P, Garcia V, et al. 2006. Transcriptome analysis of bud burst in sessile oak (*Quercus petraea*). *New Phytologist* **170**: 723–738.

Eckstein D. 2004. Change in past environments–secrets of the tree hydrosystem. *New Phytologist* **163**: 1–4.

Eckstein D. 2013. "A new star" – but why just parenchyma for dendroclimatology? *New Phytologist* **198**: 328–330.

Enquist BJ, Leffler JA. 2001. Long-term tree ring chronologies from sympatric tropical dry-forest trees: individualistic responses to climatic variation. *Journal of Tropical Ecology* **17**: 41–60.

Evans MN, Schrag DP. 2004. A stable isotope-based approach to tropical dendroclimatology. *Geochimica et Cosmochimica Acta* **68**: 3295–3305.

Fauset S, Baker TR, Lewis SL, et al. 2012. Drought-induced shifts in the floristic and functional composition of tropical forests in Ghana. *Ecology Letters* **15**: 1120–1129.

Fichtler E, Helle G, Worbes M. 2010. Stable-carbon isotope time series from tropical tree rings indicate a precipitation signal. *Tree-Ring Research* **66**: 35–49.

Fonti P, von Arx G, García-González I, et al. 2010. Studying global change through investigation of the plastic responses of xylem anatomy in tree rings. *New Phytologist* **185**: 42–53.

Forrest J, Miller-Rushing AJ. 2010. Toward a synthetic understanding of the role of phenology in ecology and evolution. *Philosophical Transactions of the Royal Society B: Biological Sciences* **365**: 3101–3112.

Fu YH, Zhao H, Piao S, et al. 2015. Declining global warming effects on the phenology of spring leaf unfolding. *Nature* **526**: 104–107.

Gebrekirstos A, Bräuning A, Sass-klassen U, Mbow C. 2014. Opportunities and applications of dendrochronology in Africa. *Current Opinion in Environmental Sustainability* **6**: 48–53.

Gessler A, Ferrio JP, Hommel R, Treydte K, Werner RA, Monson RK. 2014. Invited review. Stable isotopes in tree rings : towards a mechanistic understanding of isotope fractionation and mixing processes from the leaves to the wood. *Tree Physiology* **34**: 796–818.

Heinrich I, Banks JCG. 2006. Variation in phenology, growth, and wood anatomy of *Toona sinensis* and *Toona ciliata* in relation to different environmental conditions. *International Journal of Plant Sciences* **167**: 831–841.

Helle G, Schleser GH. 2004. Beyond CO_2-fixation by Rubisco - An interpretation of ^{13}C/^{12}C variations in tree rings from novel intra-seasonal studies on broad-leaf trees. *Plant, Cell and Environment* **27**: 367–380.

Hetzer T, Bräuning A, Leuschner HH. 2014. High-resolution climatic analysis of wood anatomical features in Corsican pine from Corsica (France) using latewood tracheid profiles. *Trees - Structure and Function* **28**: 1279–1288.

Hietz P, Horsky M, Prohaska T, Lang I, Grabner M. 2015. High-resolution densitometry and elemental analysis of tropical wood. *Trees - Structure and Function* **29**: 487–497.

Holm JA, Kueppers LM, Chambers JQ. 2017. Novel tropical forests: response to global change. *New Phytologist* **213**: 988–992.

Jansen S, Kitin P, De Pauw H, Idris M, Beeckman H, Smets E. 1998. Preparation of wood specimens for transmitted light microscopy and scanning electron microscopy. *Belgian Journal of Botany* **131**: 41–49.

Krepkowski J, Bräuning A, Gebrekirstos A, Strobl S. 2010. Cambial growth dynamics and climatic control of different tree life forms in tropical mountain forest in Ethiopia. *Trees* **25**: 59–70.

Leavitt SW. 2010. Tree-ring C-H-O isotope variability and sampling. *The Science of the Total Environment* **408**: 5244–53.

Li Z-H, Labbé N, Driese SG, Grissino-Mayer HD. 2011. Micro-scale analysis of tree-ring δ¹⁸O and δ¹³C on α-cellulose spline reveals high-resolution intra-annual climate variability and tropical cyclone activity. *Chemical Geology* **284**: 138–147.

Lisi CS, Tomazello FM, Botosso PC, *et al.* 2008. Tree-ring formation, radial increment periodicity, and phenology of tree species from a seasonal semi-deciduous forest in southeast Brazil. *IAWA Journal* **29**: 189–207.

Lubini A. 1997. La végétation de la Réserve de biosphère de Luki au Mayombe (Zaïre). *Opera Botanica Belgica* **10**: 1–155.

Managave SR, Ramesh R. 2012. Handbook of environmental isotope geochemistry. In: Baskaran M, ed. *Handbook of environmental isotope geochemistry, advances in isotopes geochemistry*. Berlin: Springer-Verlag, 811–833.

Mann M, Kahle HP, Beck M, Bender BJ, Spiecker H, Backofen R. 2018. MICA: Multiple interval-based curve alignment. *SoftwareX* **7**: 53–58.

Mariaux A. 1969. La périodicité des cernes dans le bois de Limba. *Revue Bois et Forêts des Tropiques* **128**.

Mendivelso HA, Camarero JJ, Gutiérrez E, Castaño-Naranjo A. 2016. Climatic influences on leaf phenology, xylogenesis and radial stem changes at hourly to monthly scales in two tropical dry forests. *Agricultural and Forest Meteorology* **216**: 20–36.

Michelot A, Eglin T, Dufrêne E, Lelarge-Trouverie C, Damesin C. 2011. Comparison of seasonal variations in water-use efficiency calculated from the carbon isotope composition of tree rings and flux data in a temperate forest. *Plant, Cell and Environment* **34**: 230–244.

Morris H, Plavcová L, Cvecko P, *et al.* 2016. A global analysis of parenchyma tissue fractions in secondary xylem of seed plants. *New Phytologist* **209**: 1553–1565.

Ohashi S, Okada N, Nobuchi T, Siripatanadilok S, Veenin T. 2009. Detecting invisible growth rings of trees in seasonally dry forests in Thailand: isotopic and wood anatomical approaches. *Trees* **23**: 813–822.

Olano JM, Arzac A, García-Cervigón AI, von Arx G, Rozas V. 2013. New star on the stage: amount of ray parenchyma in tree rings shows a link to climate. *New Phytologist* **198**: 486–495.

Philipson WR, Ward JM, G BB. 1971. *The vascular cambium: its development and activity*. London: Chapman & Hall.

Poussart PF, Evans MN, Schrag DP. 2004. Resolving seasonality in tropical trees: multi-decade, high-resolution oxygen and carbon isotope records from Indonesia and Thailand. *Earth and Planetary Science Letters* **218**: 301–316.

Poussart PM, Myneni SCB, Lanzirotti A. 2006. Tropical dendrochemistry: a novel approach to estimate age and growth from ringless trees. *Geophysical Research Letters* **33**: L17711.

Raffelsbauer V, Spannl S, Peña K, Pucha-Cofrep D, Steppe K, Bräuning A. 2019. Tree circumference changes and species-specific growth recovery after extreme dry events in a montane rainforest in southern Ecuador. *Frontiers in Plant Science* **10**: 1–10.

Reyer CPO, Leuzinger S, Rammig A, *et al.* 2013. A plant's perspective of extremes: Terrestrial plant responses to changing climatic variability. *Global Change Biology* **19**: 75–89.

Roden J, Siegwolf R. 2012. Is the dual-isotope conceptual model fully operational? *Tree Physiology* **32**: 1179–1182.

Rossi S, Deslauriers A. 2007. Intra-annual time scales in tree rings. *Dendrochronologia* **25**: 75–77.

Rossi S, Deslauriers A, Anfodillo T, Carrer M. 2008. Age-dependent xylogenesis in timberline conifers. *New Phytologist* **177**: 199–208.

Ryan CM, Williams M, Grace J, Woollen E, Lehmann CER. 2017. Pre-rain green-up is ubiquitous across southern tropical Africa: implications for temporal niche separation and model representation. *New Phytologist* **213**: 625–633.

Sass-Klaassen U. 2015. Tree physiology: tracking tree carbon gain. *Nature Plants* **1**: 15175.

Schleser GH, Helle G, Lücke A, Vos H. 1999. Isotope signals as climate proxies: the role of transfer functions in the study of terrestrial archives. *Quaternary Science Reviews* **18**: 927–943.

Schmitt U, Möller R, Eckstein D. 2000. Seasonal wood formation dynamics of beech (*Fagus sylvatica* L.) and black locust (*Robinia pseudoacacia* L.) as determined by the "pinning" technique. *Journal of Applied Botany - Angewandte Botanik* **74**: 10–16.

Schneider CA, Rasband WS, Eliceiri KW. 2012. NIH Image to ImageJ : 25 years of image analysis. *Nature Methods* **9**: 671–675.

Schollaen K, Heinrich I, Helle G. 2014. UV-laser-based microscopic dissection of tree rings - a novel sampling tool for δ¹³C and δ¹⁸O studies. *New Phytologist* **201**: 1045–1055.

Seo J-W, Eckstein D, Schmitt U. 2007. The pinning method: from pinning to data preparation. *Dendrochronologia* **25**: 79–86.

Silva M dos S, Funch LS, da Silva LB. 2019. The growth ring concept: seeking a broader and unambiguous approach covering tropical species. *Biological Reviews*.

Skomarkova MV, Vaganov EA, Mund M, *et al.* 2006. Inter-annual and seasonal variability of radial growth, wood density and carbon isotope ratios in tree rings of beech (*Fagus sylvatica*) growing in Germany and Italy. *Trees - Structure and Function* **20**: 571–586.

van der Sleen P, Groenendijk P, Vlam M, *et al.* 2014. No growth stimulation of tropical trees by 150 years of CO2 fertilization but water-use efficiency increased. *Nature Geoscience* **8**: 24–28.

Sonnentag O, Hufkens K, Teshera-Sterne C, *et al.* 2012. Digital repeat photography for phenological research in forest ecosystems. *Agricultural and Forest Meteorology* **152**: 159–177.

Soudant A, Loader NJ, Bäck J, Levula J, Kljun N. 2016. Intra-annual variability of wood formation and δ¹³C in tree-rings at Hyytiälä, Finland. *Agricultural and Forest Meteorology* **224**: 17–29.

Spannl S, Volland F, Pucha D, Peters T, Cueva E, Bräuning A. 2016. Climate variability, tree increment patterns and ENSO-related carbon sequestration reduction of the tropical dry forest species *Loxopterygium huasango* of Southern Ecuador. *Trees* **30**: 1245–1258.

Stangler DF, Mann M, Kahle H-P, Rosskopf E, Fink S, Spiecker H. 2016. Spatiotemporal alignment of radial tracheid diameter profiles of submontane Norway spruce. *Dendrochronologia* **37**: 33–45.

Steppe K, Sterck F, Deslauriers A. 2015. Diel growth dynamics in tree stems : linking anatomy and ecophysiology. *Trends in Plant Science* **20**: 335–343.

Tarelkin Y, Delvaux C, De Ridder M, El Berkani T, De Cannière C, Beeckman H. 2016. Growth-ring distinctness and boundary anatomy variability in tropical trees. *IAWA Journal* **37**: 275-S7.

Trouet V, Mukelabai M, Verheyden A, Beeckman H. 2012. Cambial growth season of brevi-deciduous *Brachystegia spiciformis* trees from south central Africa restricted to less than four months. *PLoS ONE* **7**: e47364.

Vaganov EA, Schulze E-D, Skomarkova MV, Knohl A, Brand WA, Roscher C. 2009. Intra-annual variability of anatomical structure and δ¹³C values within tree rings of spruce and pine in alpine, temperate and boreal Europe. *Oecologia* **161**: 729–745.

Van Camp J, Hubeau M, Van Den Bulcke J, Van Acker J, Steppe K. 2018. Cambial pinning relates wood anatomy to ecophysiology in the African tropical tree *Maesopsis eminii*. *Tree Physiology* **38**: 232–242.

Verheyden A, Kairo Gitundu J, Beeckman H, Koedam N. 2004. Growth rings, growth ring formation and age determination in the mangrove *Rhizophora mucronata*. *Annals of Botany* **94**: 59–66.

Visser ME, Caro SP, van Oers K, Schaper SV, Helm B. 2010. Phenology, seasonal timing and circannual rhythms: towards a unified framework. *Philosophical Transactions of the Royal Society B: Biological Sciences* **365**: 3113–3127.

Wieloch T, Helle G, Heinrich I, Voigt M, Schyma P. 2011. A novel device for batch-wise isolation of α-cellulose from small-amount wholewood samples. *Dendrochronologia* **29**: 115–117.

Wimmer R, Downes GM, Evans R. 2002. High-resolution analysis of radial growth and wood density in *Eucalyptus nitens*, grown under different irrigation regimes. *Annals of Forest Sciences* **59**: 519–524.

Wolfe BT, Kursar TA. 2015. Diverse patterns of stored water use among saplings in seasonally dry tropical forests. *Oecologia* **179**: 925–936.

Yáñez-Espinosa L, Terrazas T, López-Mata L. 2010. Phenology and radial stem growth periodicity in evergreen subtropical rainforest trees. *IAWA Journal* **31**: 293–307.

Zuidema PA, Baker PJ, Groenendijk P, *et al.* 2013. Tropical forests and global change: filling knowledge gaps. *Trends in Plant Science* **18**: 413–419.